ONLINE DATA SUPPLEMENT

Carbonic Anhydrase Inhibition Ameliorates Inflammation and Experimental Pulmonary Hypertension

Hannes Hudalla, MD*; Zoe Michael, MD*; Nicolas Christodoulou; Gareth R. Willis, PhD; Angeles Fernandez-Gonzalez, PhD; Evgenia J. Filatava; Paul Dieffenbach, MD; Laura E. Fredenburgh, MD; Robert S. Stearman, PhD; Mark W. Geraci, MD; Stella Kourembanas, MD; Helen Christou, MD

DETAILED METHODS

Human tissues (continued). Human samples were obtained through the Pulmonary Hypertension Breakthrough Initiative (PHBI), which is created to accrue lung tissues from patients with PAH listed for lung transplantation and controls (failed organ donors serving as normotensive controls). Funding for the PHBI is provided under an NHLBI R24 grant, #R24HL123767, and by the Cardiovascular Medical Research and Education Fund (CMREF). The organization of PHBI is outlined at http://www.ipahresearch.org. A standardized tissue processing protocol was previously described (1), peripheral lung and pulmonary artery tissues were snap frozen and obtained in RNAlater. All samples were de-identified, coded and matched for age and gender as closely as possible. Patient information is provided in Tables E2 and E3.

Animals. Adult (12-week-old) male Sprague-Dawley rats (250 to 300 g) were purchased from Charles River Laboratories (Wilmington, MA) and left to acclimatize for 2-3 days prior to experiments. Rats were housed in the animal facility at a 12:12 hrs light/dark cycle, at 22 ± 1°C ambient temperature and maintained on *ad libitum* normal Purina Rodent Chow (Purina, St. Louis, MO) and water. All animal experiments were approved by the Harvard Institutional Animal Care and Use Committee and the Harvard Medical Area Standard Committee on Animals (Brigham and Women's Institutional Animal Care and Use Committee).

Treatment protocols. Rats were randomized into different experimental groups. Acetazolamide (Spectrum, Gardena CA) (ACTZ, 1.7 mg/ml) or ammonium chloride (Sigma, St. Louis, MO) (NH_4Cl, 1.5% w/v) were added to the drinking water. Sucrose (5% w/v) was added to treated and

control animals to increase water intake. Water consumption was monitored and estimated to be ~20 ml per rat per diem. Treatment protocols were as follows: a) Early intervention SU/Hx, treatment with ACTZ or NH_4Cl from day 7 to day 24 and b) Late or Reversal SU/Hx, treatment with ACTZ from day 28 to day 49 (highlighted in Fig. 1 and 2). Experimental groups: Ctrl (normoxia control with corresponding vehicle injection), SU/Hx (Sugen/Hypoxia), SU/Hx+ACTZ (Sugen/Hypoxia treated with ACTZ), SU/Hx+NH_4Cl (Sugen/Hypoxia treated with NH_4Cl). We also treated normoxic controls with ACTZ or NH_4Cl at the same dose and for the same time period.

Hemodynamic and ventricular hypertrophy measurements. Hemodynamic measurements were performed as previously described (2). In brief, animals were anesthetized with 3% isoflurane inhalation, intubated through a tracheotomy and mechanically ventilated on a rodent ventilator (Harvard Apparatus, tidal volume 1 ml/100 g body weight, 60 breaths per minute). The thoracic cavity was opened by incision of the diaphragm. A 23-gauge butterfly needle with tubing attached to a pressure transducer was inserted first into the right ventricle and then into the left ventricle and pressure measurements were recorded with PowerLab monitoring hardware and software (ADInstruments, Colorado Springs, CO). Mean right ventricular systolic pressure (RVSP) and left ventricular systolic pressure (LVSP) (in mmHg) over the first 10 stable heartbeats were recorded. In a subset of 20 animals (5 control, 9 Su/Hx and 6 SU/Hx/ACTZ) we used a 1.2Fr Millar catheter to perform Pulmonary Artery Pressure (PAP) measurements at the Cardiovascular Physiology Core laboratory at Brigham and Women's Hospital using a similar open chest approach and a small incision in the right ventricle. We used these measurements to define the relationship between RVSP and mPAP and then calculated mPAP for all experimental animals (mPAP=0.53RVSP+2.3) (r^2=0.92). Right ventricular hypertrophy (RVH) was assessed by

weighing RV mass and expressed as Fulton's Index (FI, ratio of right ventricular weight to the left ventricular+septal weight) or as the ratio of right ventricular weight to total body weight (RV/BW).

Blood sampling. 300 µl arterial blood was collected for blood gas analysis (pH, pCO_2, HCO_3^-, BE) using a blood gas analyzer (Siemens Rapidlab1240). Two ml of blood were sampled into an EDTA-coated tube. Blood was centrifuged at 1000 × g for 20 min at 4°C within 30 min of collection and stored at -80 °C until further analysis.

Lung histology and morphometric analysis. In a subset of experimental animals, lungs were inflated by perfusing the trachea with cold 4% paraformaldehyde (PFA), excised, and fixed in 4% PFA overnight at 4° C followed by paraffin embedding. Lung sections (6 µm) were stained with hematoxylin and eosin and examined with light microscopy. Images of the arterioles were captured with a microscope digital camera system (Nikon) and analyzed using ImageJ (NIH, USA). Arterioles of comparable size (50-100 µm diameter) per rat, from the lungs of 5 different rats from each experimental group were evaluated. The percent wall thickness was determined by dividing the area occupied by the vessel wall by the total cross sectional area of the arteriole as previously reported (3). This method accounts for uneven vessel wall thickness and areas that have obliquely sectioned pulmonary arterioles.

RNA isolation and gene expression analysis. RNA isolation, analysis and reporting followed MIQE (minimum information for publication of quantitative real-time PCR experiments) criteria (4). RNA was isolated using TRIzol reagent (Invitrogen, Carlsbad, CA) per manufacturer's instructions. Yield and quality of RNA was assessed using a NanoDrop 2000c spectrophotometer

(NanoDrop Technologies) and RNA quality of human samples was further ensured by Bioanalyzer analysis (Agilent 2100 Bioanalyzer). 1 µg of RNA was treated with DNAse I (Sigma) to digest genomic DNA and poly(A)$^+$ RNA was transcribed to 20 µl complementary DNA (cDNA) using the SuperScript III First-Strand Synthesis System (Invitrogen). Relative mRNA transcript levels were analyzed with a StepOnePlus RT-PCR cycler (Applied Biosystems) using iTaq Universal SYBR Green Supermix (Bio-Rad, Hercules, CA). Primers were designed across exon-exon junctions and were specific for all transcript variants where possible using nBLAST (NCBI) and PrimerQuest Tool (Integrated DNA Technologies, IDT) and ordered through IDT. Nucleoporin 133 (Nup133), ribosomal protein S9 (Rps9) or a combination of both were used as reference genes for input normalization. Reference genes were validated for each individual tissue and cell type. Expression was analyzed with the comparative Ct method (5). Ct values were normalized to that of reference genes using the equation $\Delta Ct = Ct_{reference} - Ct_{target}$. To adequately represent downregulated genes in pulmonary arteries (PAs) and pulmonary artery smooth muscle cells (PASMCs), gene expression is displayed as ΔCt (relative mRNA expression) with the average of control samples defined as 1. Upregulated genes are shown as $2^{\Delta Ct}$ (mRNA fold change) with the average of control samples set as 1. The primers used in this study are shown in Tables E4 and E5.

Pulmonary artery and smooth muscle cell isolation. The right and left PA were dissected as distally as possible by gently pulling peripheral intrapulmonary vessels out of the parenchyma and cleaned of adventitia. PAs were then opened with a lengthwise incision and endothelium was carefully removed with a sterile cotton swab. Samples were used for protein and RNA analysis or further processed for primary PASMC culture. PAs were cut into small pieces, enzymatically digested using 1 mg/ml collagenase Type I (Worthington Biochemical Corporation, Lakewood,

NJ) and 0.125 mg/ml elastase Type III (Sigma) for 90 min at 37 ºC on a shaker and passed through a 70 μm cell strainer. PASMCs were grown in DMEM (Invitrogen) supplemented with 20% fetal bovine serum (FBS) (Atlanta Biologicals, Flowery Branch, GA), 2 mM L-glutamine (Corning, Massanas, VA) to reach a final L-glutamine concentration of 6 mM, 100 IU/ml penicillin and 100 μg/ml streptomycin (Sigma) on 0.1% gelatin-coated dishes. After the first passage, cells were grown in the same media with 10% FBS supplementation and used up to passage 3 (P3) without freezing. For each independent *in vitro* experiment cells from an individual animal were used. Cells were serum-deprived (0.5% FBS) for 48 hrs to arrest cell cycle progression at sub-confluence prior to any experiment.

PASMC proliferation assay. Primary rat PASMCs (7×10^4) were cultured in 2 ml media per well in 6-well culture dishes and serum-deprived for 48 hrs prior to stimulation with 20% serum. In some experiments cells were treated with ± 10 ng/ml rat TNFα (Sigma) and exposed to 500 μM ACTZ or media buffered to pH 6.8. In other experiments baseline differences between PASMC proliferation from the 3 experimental groups (control, SU/Hx, or SU/Hx+ACTZ animals) were compared. Cell numbers were assessed with a hemocytometer using trypan blue cell exclusion 1, 2 and 3 days after stimulation in triplicates. No difference in cell viability was seen.

Bronchoalveolar lavage and alveolar macrophage isolation. Bronchoalveolar lavage (BAL) was performed on euthanized rats as previously described (6). In brief, 16 gauge catheters were placed into the trachea and held in place by sutures. Lungs were gently flushed 4 times with 5 ml ice cold DPBS (w/o $CaCl_2$ and $MgCl_2$) and the resulting 20 ml BAL fluid was passed through a 70 μm cell strainer to remove epithelial cells, which tend to aggregate. The cellular fraction was

collected by brief centrifugation. AMs were further enriched as previously described (7) by plating cells for 6 hrs on suspension culture dishes in DMEM supplemented with 10% FBS, 100 IU/ml penicillin and 100 µg/ml streptomycin. Adherent cells were collected and their purity as AMs was confirmed by cytospin and flow cytometry. Cytospin-transferred cells were stained using PROTOCOL™ Hema 3® Stain Set (Fisher Scientific, Pittsburgh, PA) as per manufacturer's instructions showing a pure population of AMs (>99%). AM were then used directly for RNA and protein extraction.

Cytometric evaluation of alveolar macrophages from BAL. The cell suspension was stained with antibodies; PE/Cy7 conjugated-CD11b/c (BioLegend, San Diego, CA), Pacific Blue conjugated-CD11b and Alexa Flour 647 conjugated-CD68 (Bio-Rad). Fluorescence-minus-one controls were used accordingly. Flow cytometric analysis showed > 99% of cells positive for Cd68, a general macrophage marker in rats (8), and >90% positive for Cd11b/c and negative for Cd11b, characteristic for AMs (9). Flow cytometry was performed using a BD™ LSR II flow cytometer laser bench top flow cytometer, equipped with 407 nm, 488 nm and 640 nm lasers. Data was recorded using BD FACS Diva software (v 5.0.3) and analyzed using FlowJo software v10.2 (TreeStar, OR, US).

Supernatants from alveolar macrophages. 1.5×10^6 purified AMs were seeded per well in 6-well plates and cultured for 24 hr in 2 ml DMEM supplemented with 0.5% FBS, 100 IU/ml penicillin and 100 µg/ml streptomycin. Supernatant was harvested, cellular components were spun down and obtained conditioned media (CM) was frozen at -80°C. To test the potential of CM to alter PASMC phenotype, two parts of CM were mixed with 1 part of fresh vascular smooth muscle

cell culture media and a total of 2 ml were added per well onto PASMCs at sub-confluence after 48h of serum deprivation with 0.5% FBS. RNA was extracted after 24 hr of culture in CM.

Macrophage polarization assay. Bone marrow-derived macrophages (BMDMs) were obtained as previously described (6). Femur and tibia bone marrow from Sprague Dawley rats was flushed using a 10 ml syringe and passed through a 70 μm cell strainer. Cells were grown in DMEM supplemented with MCSF-enriched conditioned media from L929 cell culture, 20% serum, 100 IU/ml penicillin and 100 μg/ml streptomycin in suspension culture dishes for 7 days. Non-adherent cells were removed on day 3 and fresh media was added. After 7 days, cells were harvested and 1.5×10^6 cells were seeded in DMEM supplemented with 10% FBS, 100 IU/ml penicillin and 100 μg/ml streptomycin per well in 6-well culture dishes and left to adhere overnight. Macrophages were polarized to pro-inflammatory M1 (classically activated) with 100 ng/ml LPS from *Escherichia coli* 026:B6 (Sigma) and 20 ng/ml rat recombinant IFNγ (R&D Systems, Minneapolis, MN) or to M2 (alternatively activated) with 20 ng/ml rat recombinant IL-4 (eBioscience, San Diego, CA) and 20 ng/ml rat recombinant IL-13 (R&D Systems) for 24 hrs. Untreated macrophages served as control (M0). After 24 hrs, supernatants were collected for ELISA and RNA or protein was harvested from BMDMs.

Western blotting. Western blot analysis was performed as previously described (3). Briefly, PAs, AMs and BMDMs were homogenized in SDS lysis buffer containing cOmplete™protease inhibitor (Roche, Indianapolis, IN) and protein concentration was determined by Bradford assay (Bio-Rad). Proteins were separated by 10% Tris SDS polyacrylamide gel electrophoresis and transferred to nitrocellulose membranes (Bio-Rad) using a semi-dry system (Bio-Rad).

Membranes were blocked with 5% w/v non-fat dry milk, incubated with primary antibodies (4°C, overnight), and incubated with secondary antibodies at room temperature for 1 hr. Proteins were detected by HRP-chemiluminescence and lanes were quantified by densitometric analysis using ImageJ analysis software. An antibody against CA2 (1:400; H-70, sc-25596) was purchased from Santa Cruz (Dallas, TX). The β-Actin antibody (1:5000; AC-15) was purchased from Sigma and was used as a loading control.

Cytokine ELISA. Plasma and BMDM supernatant IL-6 levels and BMDM supernatant TNFα levels were determined with commercially available rat Quantikine sandwich ELISA kits (R6000B & RTA00; R&D Systems) as per manufacturer's instructions with minor modifications. Plasma samples were assayed undiluted (as opposed to a suggested 1:1 dilution). Cytokine concentrations were determined with a SpectraMax M2 microplate reader (Molecular Devices, Sunnyvale, CA).

Reagents. In both BMDMs and PASMCs the effect of carbonic anhydrase inhibitors and extracellular acidosis were assessed. ACTZ (Spectrum, Gardena CA) and 6-Ethoxy-2-benzothiazolesulfonamide (ethoxzolamide, EZA) (Sigma) were reconstituted in DMSO and used in different concentrations. Non-hypercapnic extracellular acidosis was induced by reducing bicarbonate concentration in the culture media to mimic *in vivo* effects of ACTZ and NH_4Cl. DMEM/F-12 media (Gibco, Gaithersburg, MD) w/o $NaHCO_3$ was supplemented with 29, 12 or 6 mM $NaHCO_3$ (Mediatech, Manassas, CA) to reach a pH of 7.4, 7.0 and 6.8 respectively in 5% CO_2 environment. The pH was determined using a pH-meter (Orion 266S) and was stable over at least 48 hrs. The physiologic relevance of this range of extracellular pH is supported by previous

in vitro studies and falls within the range of values that have been measured in tissues *in vivo* and *ex vivo*.(10)(11)(12)(13)(14)(15)(16, 17)(18)(19)(20)(21)(22)

Recombinant rat TNFα (Sigma) or IL-1β (R&D Systems) was used for PASMC de-differentiation experiments at a concentration of 10 ng/ml.

SUPPLEMENTAL FIGURES AND FIGURE LEGENDS

Fig. E1

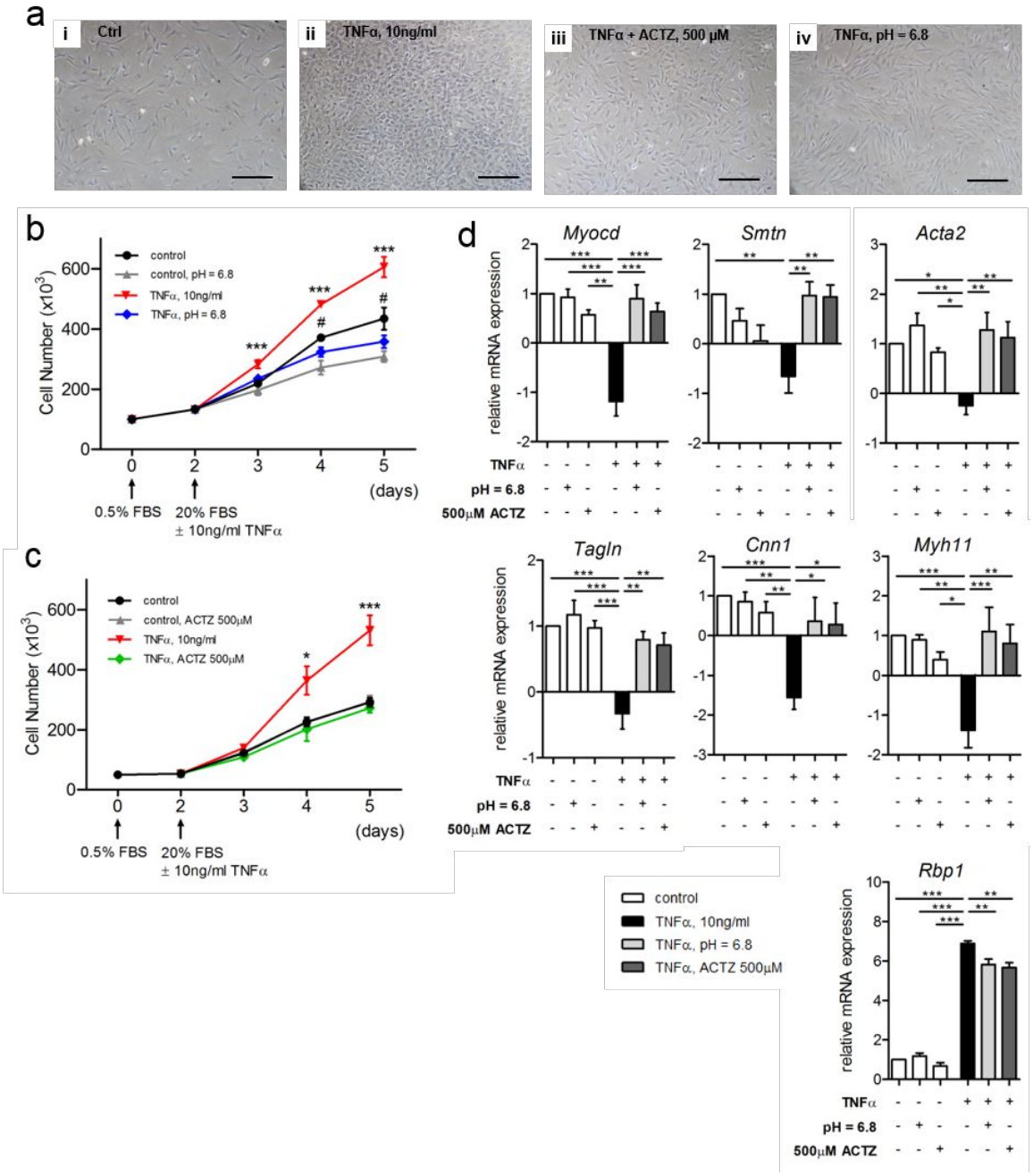

Figure E1- ACTZ and acidosis inhibit PASMCs de-differentiation *in vitro.*

(a) TNFα drives morphological de-differentiation and proliferation of PASMCs and extracellular acidosis or ACTZ ameliorate this effect. Representative microscopic images of PASMCs

stimulated with TNFα (10 ng/ml) for 48h at pH 7.4 or 6.8 or in the presence of 500 μM ACTZ. Scale bars are 400 μm. **(b)** PASMC proliferation is significantly higher after stimulation with 20% FBS and 10 ng/ml TNFα compared to 20% FBS alone and extracellular acidosis inhibits proliferation assessed by cell counts. n = 4 independent experiments. Significant difference to all other groups (*) or to control, pH 6.8 (#). **(c)** TNFα-induced PASMC proliferation is inhibited by 500 μM ACTZ. n = 3 independent experiments. Significant difference to all other groups (*). **(d)** ACTZ and extracellular acidosis partially restore a contractile phenotype of PASMCs after TNFα–induced de-differentiation. mRNA expression analysis of markers associated with a contractile or synthetic (Rbp1) PASMC phenotype after 24h of ± extracellular acidosis (pH 6.8) or ± ACTZ (500 μM) in the presence or absence of TNFα (10 ng/ml). n = 5 independent experiments. **(b-d)** Data presented as mean ± SEM. Statistical analysis by one-way ANOVA and Tukey's *post hoc* test. (* # $P < 0.05$, ** $P < 0.01$, *** $P < 0.001$).

Fig. E2

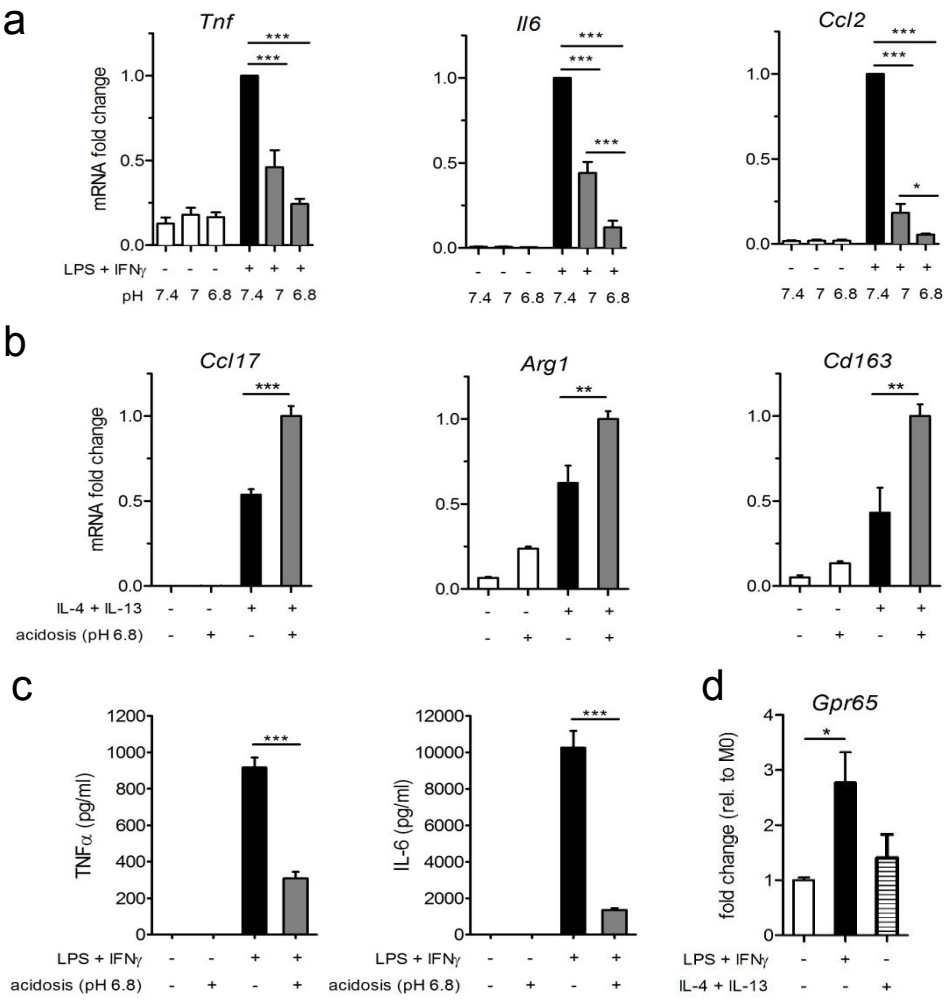

Figure E2- The effect of extracellular acidosis on BMDM polarization in vitro.

BMDM were polarized to M1 or M2 at different pH for 24 h. **(a)** Acidosis suppresses markers of M1 polarization (Tnf, Il6, Ccl2) in a pH-dependent manner assessed by qPCR. **(b)** Acidosis significantly promotes the expression of M2 polarization markers (Ccl17, Arg1, Cd163). **(c)** Acidosis significantly reduces TNFα and IL-6 secretion by M1 polarized BMDMs, measured by ELISA in BMDM supernatants. No detectable TNFα or IL-6 in M0 control macrophage supernatants. **(d)** M1 but not M2 polarization in BMDMs is associated with increased levels of

Gpr65 mRNA **(a-d)** Data presented as mean ± SEM from at least 3 independent experiments. Statistical analysis by one-way ANOVA and Tukey's *post hoc* test. Asterisks represent level of significance between groups (* $P < 0.05$, ** $P < 0.01$, *** $P < 0.001$).

Fig. E3

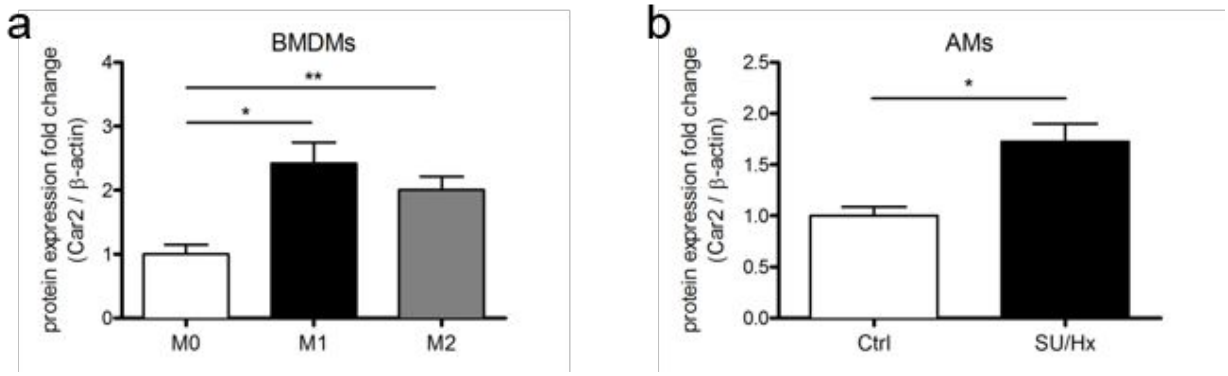

Figure E3- Quantification of westerns blots.

Protein expression levels were quantified from scanned western blots and normalized to the expression of β-actin. Expression of a control group was set as 1. **(a)** Car2 protein level in M0, M1- and M2-polarized BMDMs (Fig. 6d). n = 4 animals per experimental condition. Statistical analysis by one-way ANOVA and Tukey's *post hoc* test. **(b)** Car2 protein level in AMs from control and SU/Hx animals (Fig. 7c). n = 3 animals per group. Statistical analysis by Student's t-test. Data presented as mean ± SEM. Asterisks represent level of significance between groups (* $P < 0.05$, ** $P < 0.01$).

SUPPLEMENTAL REFERENCES

E1. Stacher E, Graham BB, Hunt JM, Gandjeva A, Groshong SD, McLaughlin VV, Jessup M, Grizzle WE, Aldred MA, Cool CD, Tuder RM. Modern age pathology of pulmonary arterial hypertension. *American journal of respiratory and critical care medicine* 2012; 186: 261-272.

2. Christou H, Reslan OM, Mam V, Tanbe AF, Vitali SH, Touma M, Arons E, Mitsialis SA, Kourembanas S, Khalil RA. Improved pulmonary vascular reactivity and decreased hypertrophic remodeling during nonhypercapnic acidosis in experimental pulmonary hypertension. *Am J Physiol Lung Cell Mol Physiol* 2012; 302: L875-890.

3. Christou H, Morita T, Hsieh CM, Koike H, Arkonac B, Perrella MA, Kourembanas S. Prevention of hypoxia-induced pulmonary hypertension by enhancement of endogenous heme oxygenase-1 in the rat. *Circ Res* 2000; 86: 1224-1229.

4. Bustin SA, Benes V, Garson JA, Hellemans J, Huggett J, Kubista M, Mueller R, Nolan T, Pfaffl MW, Shipley GL, Vandesompele J, Wittwer CT. The MIQE guidelines: minimum information for publication of quantitative real-time PCR experiments. *Clinical chemistry* 2009; 55: 611-622.

5. Schmittgen TD, Livak KJ. Analyzing real-time PCR data by the comparative C(T) method. *Nature protocols* 2008; 3: 1101-1108.

6. Zhang X, Goncalves R, Mosser DM. The isolation and characterization of murine macrophages. *Curr Protoc Immunol* 2008; Chapter 14: Unit 14 11.

7. Tian W, Jiang X, Tamosiuniene R, Sung YK, Qian J, Dhillon G, Gera L, Farkas L, Rabinovitch M, Zamanian RT, Inayathullah M, Fridlib M, Rajadas J, Peters-Golden M, Voelkel NF, Nicolls MR. Blocking macrophage leukotriene b4 prevents endothelial injury and reverses pulmonary hypertension. *Science translational medicine* 2013; 5: 200ra117.

8. Damoiseaux JG, Döpp EA, Calame W, Chao D, MacPherson GG, Dijkstra CD. Rat macrophage lysosomal membrane antigen recognized by monoclonal antibody ED1. *Immunology* 1994; 83: 140-147.

9. Barnett-Vanes A, Sharrock A, Birrell MA, Rankin S. A Single 9-Colour Flow Cytometric Method to Characterise Major Leukocyte Populations in the Rat: Validation in a Model of LPS-Induced Pulmonary Inflammation. *PloS one* 2016; 11: e0142520.

10. Galley HF, Webster NR. Acidosis and tissue hypoxia in the critically ill: how to measure it and what does it mean. *Crit Rev Clin Lab Sci* 1999; 36: 35-60.

11. Wike-Hooley JL, Haveman J, Reinhold HS. The relevance of tumour pH to the treatment of malignant disease. *Radiother Oncol* 1984; 2: 343-366.

12. Woo YC, Park SS, Subieta AR, Brennan TJ. Changes in tissue pH and temperature after incision indicate acidosis may contribute to postoperative pain. *Anesthesiology* 2004; 101: 468-475.

13. Laffey JG, Engelberts D, Kavanagh BP. Buffering hypercapnic acidosis worsens acute lung injury. *American journal of respiratory and critical care medicine* 2000; 161: 141-146.

14. Feifel E, Obexer P, Andratsch M, Euler S, Taylor L, Tang A, Wei Y, Schramek H, Curthoys NP, Gstraunthaler G. p38 MAPK mediates acid-induced transcription of PEPCK in LLC-PK(1)-FBPase(+) cells. *Am J Physiol Renal Physiol* 2002; 283: F678-688.

15. Haas MJ, Reinacher D, Li JP, Wong NC, Mooradian AD. Regulation of apoA1 gene expression with acidosis: requirement for a transcriptional repressor. *J Mol Endocrinol* 2001; 27: 43-57.
16. Terminella C, Tollefson K, Kroczynski J, Pelli J, Cutaia M. Inhibition of apoptosis in pulmonary endothelial cells by altered pH, mitochondrial function, and ATP supply. *Am J Physiol Lung Cell Mol Physiol* 2002; 283: L1291-1302.
17. Agullo L, Garcia-Dorado D, Escalona N, Inserte J, Ruiz-Meana M, Barrabes JA, Mirabet M, Pina P, Soler-Soler J. Hypoxia and acidosis impair cGMP synthesis in microvascular coronary endothelial cells. *American journal of physiology* 2002; 283: H917-925.
18. Vittone L, Mundina-Weilenmann C, Said M, Mattiazzi A. Mechanisms involved in the acidosis enhancement of the isoproterenol-induced phosphorylation of phospholamban in the intact heart. *The Journal of biological chemistry* 1998; 273: 9804-9811.
19. Ishizaka H, Kuo L. Acidosis-Induced Coronary Arteriolar Dilation is Mediated by ATP-Sensitive Potassium Channels in Vascular Smooth Muscle. *Circulation Research* 1996; 78: 50-57.
20. Berger MG, Vandier C, Bonnet P, Jackson WF, Rusch NJ. Intracellular acidosis differentially regulates KV channels in coronary and pulmonary vascular muscle. *The American journal of physiology* 1998; 275: H1351-1359.
21. Austin C, Wray S. Interactions between Ca(2+) and H(+) and functional consequences in vascular smooth muscle. *Circ Res* 2000; 86: 355-363.
22. Pilon-Thomas S, Kodumudi KN, El-Kenawi AE, Russell S, Weber AM, Luddy K, Damaghi M, Wojtkowiak JW, Mule JJ, Ibrahim-Hashim A, Gillies RJ. Neutralization of Tumor Acidity Improves Antitumor Responses to Immunotherapy. *Cancer Res* 2016; 76: 1381-1390.

SUPPLEMENTAL TABLES

Table E1. Arterial blood gases in control and intervention groups.

	Group	pH	HCO_3^- (mmol/L)	BE (mmol/L)	pCO_2 (mmHg)
	Ctrl	7.40 ± 0.01	26.9 ± 0.5	2.0 ± 0.4	43.8 ± 2.9
Early Intervention	SU/Hx	7.35 ± 0.03	24.1 ± 1.6	0.1 ± 1.2	35.3 ± 2.8
	SU/Hx + ACTZ	7.21 ± 0.03 *	17.7 ± 1.1 *	-5.5 ± 1.8 *	35.4 ± 2.2
	SU/Hx + NH_4Cl	7.08 ± 0.06 * †	13.5 ± 1.5 *	-11.5 ± 1.9 * †	33.8 ± 6.8
Reversal	SU/Hx	7.42 ± 0.02	27.3 ± 1.0	2.2 ± 0.5	52.6 ± 5.0
	SU/Hx + ACTZ	7.35 ± 0.01 *	24.1 ± 0.6 *	-2.9 ± 0.6 *	51.8 ± 2.1

Experimental groups: Ctrl (normoxia control with corresponding vehicle injection), SU/Hx (Sugen/Hypoxia untreated; early intervention or reversal), SU/Hx+ACTZ (Sugen/Hypoxia treated with ACTZ; early intervention or reversal), SU/Hx+NH_4Cl (Sugen/Hypoxia treated with NH_4Cl). BE (base excess). Data represent mean ± SEM (n = 5-24). Statistical analysis by ANOVA and Tukey's post-test. * indicates significantly ($P < 0.05$) lower pH, HCO_3^- and BE to corresponding untreated group. † indicates significantly lower pH and BE compared to SU/Hx + ACTZ. No significant differences for pCO_2.

Table E2. Patient characteristics and hemodynamic measurements for donor subjects and IPAH patients of analyzed lung tissues

Group	Sex *(M/F)*	Age *(yr)*	Race	Type of lethal injury	Reason for no lung transplant
Donor	M	17	W	drug intoxication	no recipient found
Donor	M	25	W	gunshot wound (head)	pneumothorax
Donor	M	25	W	intracranial hemorrhage	no recipient found
Donor[A]	M	41	W	gunshot wound (head)	no recipient found
Donor	M	45	W	anoxia	poor organ quality
Donor	M	51	W	CVA	poor organ function
Donor	F	28	W	motor vehicle accident	lung contusion
Donor	F	33	W	head trauma (blunt)	lung contusion
Donor	F	41	W	CVA	hypoxemia
Donor	F	56	W	CVA	poor organ function
Donor	F	57	W	CVA	poor organ function
Donor	F	60	W	CVA	lung nodule

Group	Sex *(M/F)*	Age *(yr)*	Race	NYHA class	WHO class	Systolic PAP *(mmHg)*	Diastolic PAP *(mmHg)*	mPAP *(mmHg)*	PVR[1] *(Wood Units)*	CO[1] *(L/min)*	Genetic mutation	Vasodilators
IPAH	M	16	W	III	III	78	53	63	20.5	3.08		E, Ta
IPAH	M	25	W	III	IV	113	70	88	21.48	2.7		B, E, S
IPAH	M	25	W	IV	IV	94	42	59	9.04	5.2	SMAD9	E, S, T
IPAH[B]	M	40	W	IV	IV	118	49	73	-	4.4		A, S, T
IPAH	M	45	W	-	-	66	30	48	11.08	3.25		B, E, S, T
IPAH[C]	M	51	W	IV	-	41	19	30	6.09	4.6		E, S
IPAH[D]	F	29	W	IV	III	110	49	69	12.11	4.13	BMPR2	B, I, S, T
IPAH	F	33	W	III	III	84	40	58	17.98	2.48		E, I, B
IPAH	F	41	W	IV	III	75	43	55	9.84	3.86		B, E, S
IPAH[E]	F	56	W	IV	IV	83	39	57	11.41	4.12		A, S, T
IPAH	F	57	W	III	III	119	61	82	27.27	3.22		A, B, E, S
IPAH	F	60	W	IV	IV	84	43	56	8.15	5.4		B, E, S, T

Abbreviations: CO = cardiac output, CVA = cerebrovascular accident, F = female, M = male, PAP = pulmonary arterial pressure, PVR = pulmonary vascular resistance, W = white. *N* = 12 per group.
[A-E] Marked donors or patients were used both for the analysis of lung and pulmonary artery tissue (see also Table E3). Individual patients marked in both tables by the same letter.[1] PVR and CO calculated by Fick method.
Vasodilator use: A: Ambrisentan, B: Bosentan, E: Epoprostenol, I: Iloprost, S: Sildenafil, Ta: Tadalafil, T:Treprostinil

Table E3. Patient characteristics and hemodynamic measurements for donor subjects and IPAH patients of analyzed pulmonary arteries

Group	Sex *(M/F)*	Age *(yr)*	Race	Type of lethal injury	Reason for no lung transplant
Donor	M	24	W	CVA	poor organ function
Donor[A]	M	41	W	gunshot wound (head)	no recipient found
Donor	M	47	W	Motor vehicle accident	unclear nodules in lung
Donor	M	52	W	CVA	poor organ function
Donor	M	58	W	cardiogenic shock	no recipient found
Donor	F	48	W	CVA	poor organ quality
Donor	F	50	W	CVA	poor organ quality
Donor	F	60	W	CVA	age of donor

Group	Sex *(M/F)*	Age *(yr)*	Race	NYHA class	WHO class	Systolic PAP *(mmHg)*	Diastolic PAP *(mmHg)*	mPAP *(mmHg)*	PVR[1] *(Wood Units)*	CO[1] *(L/min)*	Genetic mutation
IPAH[B]	M	40	W	IV	IV	118	49	73	-	4.4	
IPAH[C]	M	51	W	IV	-	41	19	30	6.09	4.6	
IPAH[D]	F	29	W	IV	III	110	49	69	12.11	4.13	BMPR2
IPAH	F	30	AA	III	III	63	29	41	-	-	
IPAH	F	41	H	IV	IV	72	21	43	-	-	SMAD9
IPAH[E]	F	56	W	IV	IV	83	39	57	11.41	4.12	

Abbreviations: AA = African American, CO = cardiac output, F = female, H = Hispanic, M = male, PAP = pulmonary arterial pressure, PVR = pulmonary vascular resistance, W = white. $N_{Donor} = 8$, $N_{IPAH} = 6$.
[A-E] Donor or patient samples also used for analysis of lung tissue (Table E2), marked by individual letters.[1] PVR and CO calculated by Fick method.

Table E4. Primers for rat genes in quantitative real-time PCR

Gene	Species	Accession No.	Forward Primer	Reverse Primer
Acta2	rat	NM_031004.2	5'-CTGGACGTACAACTGGTATTG-3'	5'-ATGAGGTAGTCGGTGAGAT-3'
Arg1	rat	NM_017134.3	5'-CAAGACAGGGCTACTTTCAG-3'	5'-GATTACCTTCCCGTTTCGTT-3'
Car1	rat	NM_001107660.1	5'-CAGTCAGTGCTGAAAGGTG-3'	5'-CATCCACGGTGTGTTCAG-3'
Car2	rat	NM_019291.1	5'-CTCAGTGGCTCCTACAGATT-3'	5'-GTGAACCAAGTGAAGCTCTG-3'
Car4	rat	NM_019174.3	5'-GAAACTGTCTGCCTACTTCC-3'	5'-CCAGGAACTGGTCTTTATGG-3'
Car8	rat	NM_001009662.1	5'-CCCAGCTGCAGATAGAAGAA-3'	5'-GCTGGGTAGGTCGGAAATTA-3'
Car12	rat	NM_001080756.1	5'-GATGGCCATTCAGTGAGAC-3'	5'-CCACTCACAGTGTGTTCAG-3'
Car13	rat	NM_001134993.1	5'-GAGCACAACGGTCCTATTC-3'	5'-CGGAGTGAGGAGTCGTATT-3'
Ccl2	rat	NM_031530.1	5'-CTCAGCCAGATGCAGTTAAT-3'	5'-CTGCTGGTGATTCTCTTGTAG-3'
Ccl17	rat	NM_057151.1	5'-GTGCTGCCTGGACTACTT-3'	5'-GACAGTCTCAAACACGATGG-3'
Ccnd1	rat	NM_171992.4	5'-AAGTGTGACCCGGACTG-3'	5'-AGCTTCTTCCTCCACTTCC-3'
Cd163	rat	NM_001107887.1	5'-GAAGTGCCTCCCAAGAATG-3'	5'-GGCAATGAGAAGGACCAATAG-3'
Cnn1	rat	NM_031747.1	5'-CCAGCATGGCAAAGACAA-3'	5'-CTGTAGGCCAATGATGTTCC-3'
Gpr65	rat	NM_001106751.2	5'-CCGTCTTTAACTCCATCCTTC-3'	5'-CACTTCTCCAGAGGGTATTTG-3'
Il6	rat	NM_012589.2	5'-CCCAACTTCCAATGCTCTC-3'	5'-TTGCCGAGTAGACCTCATAG-3'
Myh11	rat	NM_001170600.1	5'-GCTACAAGATCGTGAAGACC-3'	5'-GTGATGCTGCTGTCTTTCT-3'
Myocd	rat	NM_182667.2	5'-CAGTTACGGCTTCAACAGAG-3'	5'-GTCTTCAGTCTTGGCACTATC-3'
Nup133	rat	XM_008772670.2	5'-GTCTTCGATACACAAGGAGAC-3'	5'-CTTCTGCTAACAGGGACATAC-3'
Rbp1	rat	NM_012733.4	5'-TTCACCTGGAGATGAGAGC-3'	5'-TCCTCGAGACCAAGGTTATC-3'
Rps9	rat	NM_031108.4	5'-AGGTGTGGAGGGTCAAAT-3'	5'-CAGAGCGTTGCCTTCAAA-3'
Smtn	rat	NM_001013049.2	5'-GAGAACTGGCTACACTCTCA-3'	5'-AGTGTGGTCAACTCCTCTAC-3'
Tagln	rat	NM_031549.2	5'-TTATGAAGAAAGCCCAGGAG-3'	5'-CTCTGTTGCTGCCCATTT-3'
Tnf	rat	NM_012675.3	5'-GTCGTAGCAAACCACCAA-3'	5'-GAAGAGAACCTGGGAGTAGA-3'

Definition of genes: Acta2 (alpha 2 smooth muscle actin), Arg1 (arginase1), Car1 (carbonic anhydrase 1), Car2 (carbonic anhydrase 2), Car4 (carbonic anhydrase 4), Car8 (carbonic anhydrase 8), Car12 (carbonic anhydrase 12), Car13 (carbonic anhydrase 13), Ccl2 (C-C motif chemokine ligand 2 (also known as Mcp1)), Ccl17 (C-C motif chemokine ligand 17), Ccnd1 (cyclin D1), Cnn1 (calponin 1), Gpr65 (G-protein coupled receptor 65), Il6 (interleukin 6), Myh11 (myosin heavy chain 11), Myocd (myocardin), Nup133 (nucleoporin 133), Rbp1 (retinol binding protein 1), Rps9 (ribosomal protein S9), Smtn (smoothelin), Tagln (transgelin - also known as SM22), Tnf (tumor necrosis factor).

Table E5. Primers for human genes in quantitative real-time PCR

Gene	Species	Accession No.	Forward Primer	Reverse Primer
ACTA2	human	NM_001141945.2	5'-TCCTTCGTTACTACTGCTGA-3'	5'-TCTTCTCAAGGGAGGATGAG-3'
CA2	human	NM_000067.2	5'-CAAACACAACGGACCTGAG-3'	5'-CTTCAGGGAAGGGTCATACT-3'
CCL2	human	NM_002982.3	5'-CTCAGCCAGATGCAATCAA-3'	5'-CTTGCTGCTGGTGATTCTT-3'
CCND1	human	NM_053056.2	5'-CATTGAACACTTCCTCTCCA-3'	5'-GAACTTCACATCTGTGGCA-3'
CNN1	human	NM_001299.5	5'-GGAGAACATCGGCAACTTC-3'	5'-CTTTCGTCTTCGCCATGC-3'
IL6	human	NM_000600.4	5'-CATGTGTGAAAGCAGCAAAG-3'	5'-CAGGCAAGTCTCCTCATTG-3'
IL1B	human	NM_000576.2	5'-GTGTTCTCCATGTCCTTTGT-3'	5'-TTGGGATCTACACTCTCCAG-3'
MYH11	human	NM_001040113.1	5'-CTGGAAGTGCGGCTAAAG-3'	5'-GCTGCATCTTGAGCTCTG-3'
MYOCD	human	NM_001146312.2	5'-GTCCAGCTGAATTCCATGAG-3'	5'-GTGGAAGCTTGGAGTATGTG-3'
NUP133	human	NM_018230.2	5'-CAGGGAGGTATCCCAAGTAG-3'	5'-CACCACTTCAGCCCATTC-3'
RBP1	human	NM_002899.3	5'-CAGACAAAGAGATCGTGCAG-3'	5'-CACTTGCGGTCATCTATGC-3'
RPS9	human	NM_001013.3	5'-CATCCCGTCCTTCATTGTC-3'	5'-GCCCTTCTTGGCATTCTT-3'
SMTN	human	NM_134270.2	5'-CAGACCCGAGTGAACAAAG-3'	5'-GCTCTGATCCAGCATCTTG-3'
TAGLN	human	NM_001001522.1	5'-AAGAATGGCGTGATTCTGAG-3'	5'-GCTCCATCTGCTTGAAGAC-3'

Definition of genes: ACTA2 (alpha 2 smooth muscle actin), CA2 (carbonic anhydrase 2), CCL2 (C-C motif chemokine ligand 2 (also known as Mcp1)), CCND1 (cyclin D1), CNN1 (calponin 1), IL6 (interleukin 6), IL1B (interleukin 1 beta), MYH11 (myosin heavy chain 11), MYOCD (myocardin), NUP133 (nucleoporin 133), RBP1 (retinol binding protein 1), RPS9 (ribosomal protein S9), SMTN (smoothelin), TAGLN (transgelin - also known as SM22).